

# A Simple and Efficient Diffuse Interface Method for Compressible Two- Phase Flows

**2009 International Conference on  
Mathematics, Computational Methods  
& Reactor Physics**

Ray A. Berry  
Richard Saurel  
Fabien Petitpas

May 2009

The INL is a  
U.S. Department of Energy  
National Laboratory  
operated by  
Battelle Energy Alliance



This is a preprint of a paper intended for publication in a journal or proceedings. Since changes may be made before publication, this preprint should not be cited or reproduced without permission of the author. This document was prepared as an account of work sponsored by an agency of the United States Government. Neither the United States Government nor any agency thereof, or any of their employees, makes any warranty, expressed or implied, or assumes any legal liability or responsibility for any third party's use, or the results of such use, of any information, apparatus, product or process disclosed in this report, or represents that its use by such third party would not infringe privately owned rights. The views expressed in this paper are not necessarily those of the United States Government or the sponsoring agency.

# **A SIMPLE AND EFFICIENT DIFFUSE INTERFACE METHOD FOR COMPRESSIBLE TWO-PHASE FLOWS**

**Ray A. Berry**

Multiphysics Methods Group  
Idaho National Laboratory  
P.O. Box 1625, Idaho Falls, ID 83415-3840  
[Ray.Berry@inl.gov](mailto:Ray.Berry@inl.gov)

**Richard Saurel and Fabien Petitpas**

Mecanique Energetique  
Polytech'Marseille, Aix-Marseille University  
5 rue E. Fermi, 13453 Marseille Cedex 13, France  
[Richard.Saurel@polytech.univ-mrs.fr](mailto:Richard.Saurel@polytech.univ-mrs.fr); [Fabien.Petitpas@polytech.univ-mrs.fr](mailto:Fabien.Petitpas@polytech.univ-mrs.fr)

## **ABSTRACT**

In nuclear reactor safety and optimization there are key issues that rely on in-depth understanding of basic two-phase flow phenomena with heat and mass transfer. For many reasons, to be discussed, there is growing interest in the application of two-phase flow models to provide diffuse, but nevertheless resolved, simulation of interfaces between two immiscible compressible fluids – diffuse interface method (DIM). Because of its ability to dynamically create interfaces and to solve interfaces separating pure media and mixtures for DNS-like (Direct Numerical Simulation) simulations of interfacial flows, we examine the construction of a simple, robust, fast, and accurate numerical formulation for the 5-equation Kapila et al. [1] reduced two-phase model. Though apparently simple, the Kapila et al. model contains a volume fraction differential transport equation containing a nonlinear, non-conservative term which poses serious computational challenges. To circumvent the difficulties encountered with the single velocity and single pressure Kapila et al. [1] multiphase flow model, a 6-equation relaxation hyperbolic model is built to solve interface problems with compressible fluids. In this approach, pressure non-equilibrium is first restored, followed by a relaxation to an asymptotic solution which is convergent to the solutions of the Kapila et al. reduced model. The apparent complexity introduced with this extended hyperbolic model actually leads to considerable simplifications regarding numerical resolution, and the various ingredients used by this method are general enough to consider future extensions to problems involving complex physics.

*Key Words:* diffuse interface methods (DIM), compressible multiphase flow, relaxation methods, direct numerical simulation (DNS)

## **1. INTRODUCTION**

Within the context of multiphase flows, two bubble-dynamic phenomena – boiling (heterogeneous) and flashing or cavitation (homogeneous boiling), with bubble collapse, are technologically very important to nuclear reactor systems. The main difference between boiling and flashing is that bubble growth (and collapse) in boiling is inhibited by limitations on the heat transfer at the interface, whereas bubble growth (and collapse) in flashing is limited primarily by

inertial effects in the surrounding liquid. The flashing process tends to be far more explosive (and implosive), and is more violent and damaging (at least in the near term) than the bubble dynamics of boiling. However, other problematic phenomena, such as crud deposition, appear to be intimately connecting with the boiling process. In reality, these two processes share many details.

Flashing occurs in flowing liquid systems when the pressure falls sufficiently low in some region of the flow, reaching a metastable state where the temperature is higher than the saturated one at the reduced pressure of this expanded state. Then the superheated liquid releases its metastable energy (stored as internal energy) very quickly, even explosively, producing either pure vapor (bubble) or liquid-vapor mixture at high velocity, [2]. Expansion effects in nuclear reactor systems are often due to geometrical effects, as for example in nozzles where flashing appears at locations where the pressure is relatively low and the liquid superheated. In the case of two-phase blowdown (from the superheated liquid state), bubble collapse is usually not important, but the flashing of superheated liquid strongly influences critical flow rates. In other cases however, besides the performance limitations which this cavitation may cause in flow systems, subsequent bubble collapse may be responsible for damage to nearby solid surfaces.

Many nuclear reactor applications rely on convective nucleate boiling to efficiently remove high heat fluxes from heated surfaces. Nucleate boiling is a very effective heat transfer mechanism, however it is well known that there exists a critical value of the heat flux at which nucleate boiling transitions to film boiling (departure from nucleate boiling (DNB) and boiling crisis), a very poor heat transfer mechanism. In most practical applications it is imperative to maintain the operating heat flux below such critical value, which is called the Critical Heat Flux (CHF). In this case, the presence of a nearby solid surface is necessary for the rapid supply of the latent heat inherent in the phase change. The presence of these surfaces is known to modify the flow patterns and other characteristics of these multiphase flows, and therefore must be interactively coupled with analyses of these phenomena. And as mentioned above, DNB is believed to play an integral role in performance degradation as well as the crud deposition problem. Our inability to accurately predict heat transfer and heat transfer regime transitions (flow topologies) in the real nuclear reactor two-phase flow conditions and fuel bundle geometry results in increased safety margins and impedes the development of new fuel designs.

With the advent of increased available computational power and of a new generation of codes (as evidenced at the recent international “Two-phase Convective Flow Modelling” workshop [3]) it is believed that significant progress can be made by using computational fluid dynamics (CFD) for nuclear fuel design thus leading to a drastic reduction in development costs. In France, CEA, EDF, AREVA and IRSN have launched the NEPTUNE project, aimed at providing tools describing two-phase flow and heat transfer that are validated in the parameter range of the industrial applications, plus others covering the entire spectrum of space and time scales. In the U.S. no such unified effort exists, but because it seems necessary to promote collaborative research on this subject at the widest scale, the INL has embarked on such a task, though at a reduced scale.

Thus, there are key issues in nuclear reactor safety and optimization that rely on an in-depth understanding of basic two-phase flow phenomena with heat transfer and phase change. The

results discussed here derive directly from our current research aimed at developing well-designed physical/mathematical models along with high-resolution numerical solution methods for general multiphase flows. While that research is directed towards unified physical and numerical model development of multiphase mixtures in general, the work described here represents a synergistic reduction of those multiphase mixture models to DNS-like (direct numerical simulation) simulation of highly resolved interfacial phenomena important to nuclear reactor systems – boiling, flashing or cavitation of superheated liquid, and bubble collapse.

The underlying objective of the present work is the accurate and computationally efficient resolution of interface problems in compressible multiphase mixtures in all flow conditions, high pressure ratios and high density ratios, as well as the computation of dynamic appearance of interfaces, that occur in flashing flow. These interfaces are often separating pure media but also mixtures of phases in which wave dynamics is also important. The presence of large discontinuities of thermodynamic variables and equations of state at interfaces frequently results in numerical instabilities, oscillations, and computational failure. Here a general formulation and algorithm will be given to solve interface problems separating compressible media or mixtures in extreme conditions.

The literature is replete with methods purported to circumvent these difficulties, but most can be placed categorically into two classes of methods: (1) Methods that consider the interface as a sharp discontinuity, Sharp Interface Methods (SIM), and (2) Methods that consider the interface as a diffuse zone, like contact discontinuities in gas dynamics, Diffuse Interface Methods (DIM).

There are numerous methods in the SIM class, which includes Volume of Fluid (VOF), level set, and Ghost Fluid Method. The reader is referred to [4] for a summary of features/weaknesses. It is important to point out, however, that none of these methods is able to dynamically create interface, and to solve interfaces separating pure media and mixtures.

In the second type of methods (DIM), diffuse interfaces correspond to artificial mixtures, created by numerical diffusion, for which determination of thermodynamic flow variables in these zones is achieved on the basis of multiphase flow theory. The challenge is to derive physically, mathematically, and numerically consistent thermodynamic relations for the mixture, with the key issue of fulfilling correct interfacial conditions within this artificial mixture. The reader is again referred to [4] for a summary. This second category possesses several advantages:

- The same algorithm is implemented globally in both pure fluids and in mixture zones. An extended hyperbolic system is used to solve every location of the flow.
- These models and methods are able to dynamically create interfaces that are not present initially.
- These methods are also able to deal with interfaces separating pure fluids and fluid mixtures.

Methods in this second category are based on hyperbolic multiphase flow models, consisting of two main classes:

- Models for mixtures in total non-equilibrium: Baer and Nunziato model [5] and its variants, and
- Models for mixtures in mechanical equilibrium [6, 1].

In this paper, a simple, robust, fast and accurate formulation for single velocity and single pressure multiphase flows is given. The Kapila et al. model [1] is of particular interest for the computation of interfaces separating compressible fluids, as well as barotropic and non-barotropic cavitating flows. Specific numerical schemes have been derived recently in Murrone and Guillard [7], Abgrall and Perrier [8], Saurel et al. [9], Petitpas et al. [10].

This model is apparently simple. In the context of two fluids it is composed of two mass equations, a mixture momentum equation and a mixture energy equation. These equations are expressed in conservative form. The closure is achieved by the pressure equilibrium condition that results in a differential transport equation for the volume fraction containing a non conservative term, involving the velocity divergence and phasic bulk moduli. However this last equation poses serious computational challenges which include:

- Shock computations within the context of a non-conservative model.
- Volume fraction positivity, when dealing with shocks and strong expansion waves. The term involving a velocity divergence in the volume fraction evolution equation is particularly difficult to approximate [10]. This is particularly important for the dynamic appearance of interfaces in cavitating flows.
- Non-monotonic behavior of the sound speed [11] which produces multiple sonic points in the numerical diffusion zones at interfaces. As it is very difficult (and expensive) to solve exactly the Riemann problem [10], approximate Riemann solvers are used resulting in sampling errors (with multiple sonic points) in the flux computations as well as in the non-conservative equation evolution. These difficulties in the Riemann problem solution are due to volume fraction variations across shocks and expansion waves.

Moreover, in order to consider future extensions, with additional physics, within the context of multiphysics modeling of continuous media with a multiphase approach, the computational efficiency of existing algorithms must be improved. The present paper doesn't deal with these extensions, but it is clear that such a goal needs simple and robust multiphase formulations, which will be demonstrated here.

The present paper addresses this issue in the context of the simplest version of the Kapila et al. model [1]. The main difficulty with this model comes from the pressure equilibrium condition, which results in the non-conservative equation for the volume fraction. A conservative formulation can be obtained with the help of the entropy equations. However, this conservative formulation is untenable in the presence of shocks.

To circumvent these difficulties, pressure non-equilibrium effects are restored in the Kapila et al. model [1]. This results in a 6-equation model with a single velocity but with two pressures and associated relaxation terms. This extended model was previously presented as a first reduction of the Baer and Nunziato model [5] in Kapila et al. [1], but not considered for the description of diffuse interfaces. A seventh equation is added describing the mixture total energy in order to guarantee a correct treatment of shocks in the single phase limit. This apparent complexity with an extended model actually leads to considerable simplifications regarding numerical resolution. Indeed, this model remains hyperbolic with only three characteristic wave propagation speeds, volume fraction positivity is easily preserved and multiple sonic points no longer appear during hyperbolic evolution. The building of a simple and efficient method for the numerical

approximation of this flow model in the context of diffuse interfaces will be described in the present paper.

When relaxation terms are omitted the volume fraction remains constant across acoustic waves and the Riemann problem is easily solved with approximate Riemann solvers (acoustic and HLLC-type solvers [12]). With this non-equilibrium pressure model, the sound speed has a monotonic behavior versus volume fraction and multiple sonic points no longer appear inside the numerical diffusion zone at interfaces. This feature provides robustness when considering flashing or cavitating flows [13, 14, 10]. This hyperbolic step is then followed by a relaxation step that consists in the determination of the asymptotic solution of a differential problem in the limit of infinitely fast relaxation. This asymptotic solution results in resolution of an algebraic system. The combination of these two steps (hyperbolic + relaxation) guarantees convergence of the method to solutions of the Kapila et al. reduced model [1].

## 2. SIX-EQUATION, PRESSURE NON-EQUILIBRIUM, SINGLE VELOCITY, MULTIPHASE FLOW MODEL

The single velocity pressure equilibrium model corresponds to the one of Kapila et al. [1]. It has been obtained as the asymptotic limit of the Baer and Nunziato model [5] in the limit of both stiff velocity and pressure relaxation. It involves 5 partial differential equations, 2 phasic continuity equations, mixture momentum, mixture total energy, volume fraction evolution equation which is non-conservative. Its resulting speed of sound corresponds to that of Wood [11] which exhibits a non-monotonic variation with volume fraction. These two difficulties (non-conservativity and non-monotonicity) present serious computational challenges. To circumvent them, a pressure non-equilibrium 6-equation model is constructed (first reduced model in Kapila et al. [1]), also non-conservative, but easier to solve with a relaxation method. Due to space limitations the reader is referred to [4] for details.

To circumvent these difficulties and develop a simple algorithm able to deal with multiphysics extensions, a pressure non-equilibrium is considered. The 6-equation model is also derived from the 7-equation model of Baer and Nunziato [5] in the asymptotic limit of stiff velocity relaxation only (first reduced model in Kapila et al. [1]). Pressure non-equilibrium effects are maintained. The 6-equation model should not be considered as a physical model, but more as a step-model to solve the 5-equations model (second reduced model of Kapila et al. [1]). Indeed, the model with 6-equations has better properties for numerical approximations than the mechanical equilibrium one:

- Positivity of the volume fraction is easily preserved,
- The mixture sound speed has a monotonic behavior.

These two properties are key points for the construction of a simple, robust and accurate hyperbolic solver. Moreover, with proper treatment of relaxation terms, solutions of the 5-equation model will be recovered.

### Flow model

The 6-equation model is

$$\begin{aligned}
\frac{\partial \alpha_1}{\partial t} + u \frac{\partial \alpha_1}{\partial x} &= \mu(p_1 - p_2) \\
\frac{\partial \alpha_1 \rho_1}{\partial t} + \frac{\partial \alpha_1 \rho_1 u}{\partial x} &= 0 \\
\frac{\partial \alpha_2 \rho_2}{\partial t} + \frac{\partial \alpha_2 \rho_2 u}{\partial x} &= 0
\end{aligned} \tag{1}$$

$$\begin{aligned}
\frac{\partial \rho u}{\partial t} + \frac{\partial \rho u^2 + (\alpha_1 p_1 + \alpha_2 p_2)}{\partial x} &= 0 \\
\frac{\partial \alpha_1 \rho_1 e_1}{\partial t} + \frac{\partial \alpha_1 \rho_1 e_1 u}{\partial t} + \alpha_1 p_1 \frac{\partial u}{\partial x} &= -p_1 \mu(p_1 - p_2) \\
\frac{\partial \alpha_2 \rho_2 e_2}{\partial t} + \frac{\partial \alpha_2 \rho_2 e_2 u}{\partial t} + \alpha_2 p_2 \frac{\partial u}{\partial x} &= p_1 \mu(p_1 - p_2)
\end{aligned}$$

where  $\alpha_k$ ,  $\rho$ ,  $u$ ,  $p_k$ , and  $e_k$  represent respectively the volume fractions, the mixture density, the mixture velocity, the phasic pressures, and the phasic internal energies.

Each fluid is governed by its own convex equation of state (EOS). For example, in the case of fluids governed by the stiffened gas EOS

$$p_k = (\gamma_k - 1) \rho_k e_k - \gamma_k p_{\infty k}, \tag{2}$$

which allows the determination of the phases' sound speed,  $c_k = c_k(\rho_k, p_k)$ . The mixture density is defined as  $\rho = (\alpha \rho)_1 + (\alpha \rho)_2$ .

The interfacial pressure  $p_1$  is obtained as the asymptotic limit of the interfacial pressure of the symmetric non-equilibrium model with 7-equations of Saurel et al. [15]. In the limit of equal velocities, this estimate is

$$p_1 = \frac{Z_2 p_1 + Z_1 p_2}{Z_1 + Z_2},$$

where  $Z_k = \rho_k c_k$  represents the acoustic impedance of phase  $k$ .

The combination of the two internal energy equations with mass and momentum equations results in the additional mixture energy equation

$$\frac{\partial \rho(Y_1 e_1 + Y_2 e_2 + \frac{1}{2} u^2)}{\partial t} + \frac{\partial u \left( \rho(Y_1 e_1 + Y_2 e_2 + \frac{1}{2} u^2) + (\alpha_1 p_1 + \alpha_2 p_2) \right)}{\partial x} = 0 \tag{3}$$

where the mass fractions are given by  $Y_k = \frac{(\alpha \rho)_k}{\rho}$ . This additional equation will be important during numerical resolution, in order to correct inaccuracies due to the numerical approximation of the two non-conservative internal energy equations in the presence of shocks.

There is no difficulty to check that the second law of thermodynamics is fulfilled by this model. The phasic entropy equations are readily obtained as

$$\alpha_1 \rho_1 T_1 \frac{ds_1}{dt} = \mu(p_1 - p_2)^2 \frac{Z_1}{Z_1 + Z_2}$$

$$\alpha_2 \rho_2 T_2 \frac{ds_2}{dt} = \mu(p_1 - p_2)^2 \frac{Z_2}{Z_1 + Z_2},$$

insuring that the mixture entropy ( $s = Y_1 s_1 + Y_2 s_2$ ) always evolves with positive or null variations.

This model exhibits a nice feature with respect to the mixture sound speed. The mixture sound speed

$$c_f^2 = Y_1 c_1^2 + Y_2 c_2^2$$

has a monotonic behavior versus volume and mass fractions and represents the frozen mixture sound speed. The model is thus strictly hyperbolic with waves speeds  $u + c_f$ ,  $u - c_f$ , and  $u$ .

As with the 5-equation model of Kapila et al. [1], the new model is also non-conservative, and shock relations have to be prescribed. However, *even when shock relations are known or accepted for a non-conservative system, it is very difficult to make the numerical solution converge naturally to the end shock state solution.* ‘Natural convergence’ means without artifact such as artificial heat exchanges [10]. There is thus no need to determine precise shock relations for the 6-equation model, in particular since it is intended only to approximate the 5-equation model for which shock relations are known. However, some admissibility conditions have to be respected by a given Hugoniot approximate model. Jump conditions must at least respect [16]:

- Energy conservation of the mixture,
- Tangency of the mixture Hugoniot curve and mixture isentrope,
- Single phase limit for which jump conditions are unambiguously known,
- Symmetry ,
- Entropy production.

Jump conditions for the mass equations are

$$\alpha_1 \rho_1 (u - \sigma) = \alpha_1^0 \rho_1^0 (u^0 - \sigma) = m_1$$

$$\alpha_2 \rho_2 (u - \sigma) = \alpha_2^0 \rho_2^0 (u^0 - \sigma) = m_2 .$$

Denoting the mixture pressure by  $p = \alpha_1 p_1 + \alpha_2 p_2$  and the shock mass flow rate by  $m = m_1 + m_2$ , the momentum jump condition can be written

$$p - p^0 + m^2 (v - v^0) = 0 ,$$

where  $v = Y_1 v_1 + Y_2 v_2$  ( $v_k = \frac{1}{\rho_k}$ ).

The mixture energy jump condition is

$$e - e^0 + \frac{p + p^0}{2} (v - v^0) = 0 ,$$

with  $e = Y_1 e_1 + Y_2 e_2$ .

In the absence of relaxation effects the volume fraction jump is simply

$$\alpha_1 = \alpha_1^0 .$$



The non-conservative internal energy equations are not adapted to the determination of jump conditions. Following the preceding admissibility conditions the following jump conditions are proposed:

$$e_k - e_k^0 + \frac{p_k + p_k^0}{2}(v_k - v_k^0) = 0. \quad (4)$$

The conditions that must be satisfied include:

- *Energy conservation*

The mass fraction weighted sum of the internal energy jump equations yields

$$Y_1(e_1 - e_1^0) + \frac{p_1 + p_1^0}{2}(Y_1 v_1 - Y_1 v_1^0) + Y_2(e_2 - e_2^0) + \frac{p_2 + p_2^0}{2}(Y_2 v_2 - Y_2 v_2^0) = 0$$

As  $Y_k = \frac{\alpha_k v}{v_k}$ , we have:

$$e - e^0 + \frac{p_1 + p_1^0}{2}(\alpha_1 v - \alpha_1^0 v^0) + \frac{p_2 + p_2^0}{2}(\alpha_2 v - \alpha_2^0 v^0) = 0$$

With the volume fraction jump relation, this equation becomes

$$e - e^0 + \frac{\alpha_1 p_1 + \alpha_2 p_2 + \alpha_1 p_1^0 + \alpha_2 p_2^0}{2}(v - v^0) = 0,$$

or simply

$$e - e^0 + \frac{p + p^0}{2}(v - v^0) = 0.$$

This result guarantees that the phasic energy jump conditions are compatible with the mixture energy conservation.

- *Tangency of the mixture Hugoniot curve and isentrope*

This is a mandatory property for the Riemann problem solution. As the volume fraction is constant across shocks and rarefaction waves (in absence of relaxation effects) and the phasic Hugoniot are tangent to phasic isentropes, the mixture Hugoniot is necessarily tangent to the mixture isentrope.

- *Single phase limit*

When one of the phases disappears the energy jump condition of the remaining fluid is in agreement with the single phase energy jump.

- *Symmetry*

Symmetry in the formulation allows an easy extension to an arbitrary number of fluids.

- *Entropy production*

As each phase evolves along its own Hugoniot, Eqn. (4), there is no doubt that the mixture entropy evolves positively.

Through application of these relations, the Riemann problem can now be solved. Numerical issues pertaining to the Riemann solution are addressed in the next section. Let us insist on the fact that jump conditions are not the key to shock computation in multiphase mixtures. It has been shown that even when shock relations are known, the convergence of a numerical scheme to the exact solution is very difficult. This is due to the lack of definition for cell averages of non-conservative variables [10].

### Asymptotic limit

As the method will solve the 6-equation model with stiff relaxation terms, it is important to check that in the limit of infinitely fast pressure relaxation the 5-equation model is recovered. This proof is given in Appendix B of reference [4].

## 3. NUMERICAL METHOD

Numerical resolution of the 6-equation model in the limit of stiff pressure relaxation is addressed in the present section. In regular zones, this model is self-consistent. But in the presence of shocks the internal energy equations are inappropriate. To correct the thermodynamic state predicted by these equations in the presence of shocks, the total mixture energy equation will be used. This correction will be valid on both sides of an interface, when the flow tends to the single phase limits. The details of this correction will be examined further. For now, the 6-equation system is augmented by a redundant equation regarding the total mixture energy. The system to consider during numerical resolution thus involves 7 equations,

$$\begin{aligned}
\frac{\partial \alpha_1}{\partial t} + u \frac{\partial \alpha_1}{\partial x} &= \mu(p_1 - p_2) \\
\frac{\partial \alpha_1 \rho_1 e_1}{\partial t} + \frac{\partial \alpha_1 \rho_1 e_1 u}{\partial x} + \alpha_1 p_1 \frac{\partial u}{\partial x} &= -p_1 \mu(p_1 - p_2) \\
\frac{\partial \alpha_2 \rho_2 e_2}{\partial t} + \frac{\partial \alpha_2 \rho_2 e_2 u}{\partial x} + \alpha_2 p_2 \frac{\partial u}{\partial x} &= p_1 \mu(p_1 - p_2) \\
\frac{\partial \alpha_1 \rho_1}{\partial t} + \frac{\partial \alpha_1 \rho_1 u}{\partial x} &= 0 \\
\frac{\partial \alpha_2 \rho_2}{\partial t} + \frac{\partial \alpha_2 \rho_2 u}{\partial x} &= 0 \\
\frac{\partial \rho u}{\partial t} + \frac{\partial \rho u^2 + (\alpha_1 p_1 + \alpha_2 p_2)}{\partial x} &= 0 \\
\frac{\partial \rho (Y_1 e_1 + Y_2 e_2 + \frac{1}{2} u^2)}{\partial t} + \frac{\partial u \left( \rho (Y_1 e_1 + Y_2 e_2 + \frac{1}{2} u^2) + (\alpha_1 p_1 + \alpha_2 p_2) \right)}{\partial x} &= 0
\end{aligned} \tag{5}$$

with  $p_1 = \frac{Z_2 p_1 + Z_1 p_2}{Z_1 + Z_2}$  and appropriate equations of state  $e_k = e_k(\rho_k, p_k)$ .

This system is equipped with the approximate shock relations of the preceding section, in particular the relation given by Eqn. (4).

### 3.1 HLLC Type Approximate Riemann solver

The HLLC type approximate Riemann solver is detailed in the context of the Euler equations in Toro [12]. Consider a cell boundary separating a left state (L) and a right state (R). The left- and right-facing waves speeds are readily obtained, following Davis [17] estimates as

$$S_R = \max(u_L + c_L, u_R + c_R), \quad S_L = \min(u_L - c_L, u_R - c_R),$$

where the sound speed still obeys  $c^2 = Y_1 c_1^2 + Y_2 c_2^2$ . The speed of the intermediate wave (or contact discontinuity) is estimated using the HLL approximation

$$S_M = \frac{(\rho u^2 + p)_L - (\rho u^2 + p)_R - S_L(\rho u)_L + S_R(\rho u)_R}{(\rho u)_L - (\rho u)_R - S_L \rho_L + S_R \rho_R},$$

with the mixture density and mixture pressure defined previously.

From these wave speeds, the following variable states are determined

$$(\alpha_k \rho_k)_R^* = (\alpha_k \rho_k)_R \frac{S_R - u_R}{S_R - S_M},$$

$$(\alpha_k \rho_k)_L^* = (\alpha_k \rho_k)_L \frac{S_L - u_L}{S_L - S_M},$$

$$p^* = p_R + \rho_R u_R (u_R - S_R) - \rho_R^* S_M (S_M - S_R), \text{ with } \rho_R^* = \sum_k (\alpha_k \rho_k)_R^*,$$

$$E_R^* = \frac{\rho_R E_R (u_R - S_R) + p_R u_R - p^* S_M}{\rho_R^* (S_M - S_R)},$$

$$E_L^* = \frac{\rho_L E_L (u_L - S_L) + p_L u_L - p^* S_M}{\rho_L^* (S_M - S_L)}, \text{ with } E = Y_1 e_1 + Y_2 e_2 + \frac{1}{2} u^2.$$

The volume fraction jump is readily obtained, as in the absence of relaxation effects, the volume fraction is constant along fluid trajectories

$$\alpha_{kR}^* = \alpha_{kR}, \quad \alpha_{kL}^* = \alpha_{kL}.$$

As the volume fraction is constant across left- and right-facing waves, the fluid density is determined from the preceding relations to be

$$\rho_{kR}^* = \rho_{kR}^0 \frac{u_R - S_R}{S_M - S_R}$$

Internal energy jumps are determined with the help of the Hugoniot relation, Eqn. (4). Let us consider the example of fluids governed by the stiffened gas EOS, Eqn. (2). With the help of the EOS, the phasic pressures are constrained along their Hugoniot curves to be functions only of the corresponding phase density

$$p_k^*(\rho_k^*) = \left( p_k^0 + p_{\infty k} \right) \frac{(\gamma_k - 1) \rho_k^0 - (\gamma_k + 1) \rho_k^*}{(\gamma_k - 1) \rho_k^* - (\gamma_k + 1) \rho_k^0} - p_{\infty k}$$

The phase's internal energies are then determined from the EOS,  $e_{kR}^* = e_{kR}^*(p_k^*, \rho_k^*)$ .

Equipped with these approximate Riemann solvers, the next step is to develop a Godunov type scheme.

### 3.2 Godunov type method

For the sake of simplicity, the method is presented at first-order. In the absence of relaxation terms, the conservative part of system Eqns. (1) is updated with the conventional explicit Godunov scheme

$$U_i^{n+1} = U_i^n - \frac{\Delta t}{\Delta x} \left( F^*(U_i^n, U_{i+1}^n) - F^*(U_{i-1}^n, U_i^n) \right),$$

where  $U = ((\alpha\rho)_1, (\alpha\rho)_2, \rho u, \rho E)^T$  and  $F = ((\alpha\rho)_1 u, (\alpha\rho)_2 u, \rho u^2 + p, (\rho E + p)u)^T$ ,  
 $E = Y_1 e_1 + Y_2 e_2 + \frac{1}{2}u^2$  and  $p = \alpha_1 p_1 + \alpha_2 p_2$ .

The volume fraction equation is also updated using the Godunov method for advection equations

$$\alpha_{1i}^{n+1} = \alpha_{1i}^n - \frac{\Delta t}{\Delta X} \left( (u\alpha_1)_{i+1/2}^* - (u\alpha_1)_{i-1/2}^* - \alpha_{1i}^n (u_{i+1/2}^* - u_{i-1/2}^*) \right).$$

This scheme guarantees volume fraction positivity during the hyperbolic step. Regarding the non-conservative energy equations, there is no hope of determining an accurate approximation in the presence of shocks [18]. Therefore, we use the simplest approximation of the corresponding equations by assuming the product  $(\alpha\rho)_{ki}^n$  to be constant during the time step, giving

$$(\alpha\rho e)_{ki}^{n+1} = (\alpha\rho e)_{ki}^n - \frac{\Delta t}{\Delta X} \left( (\alpha\rho eu)_{ki+1/2}^* - (\alpha\rho eu)_{ki-1/2}^* + (\alpha\rho)_{ki}^n (u_{i+1/2}^* - u_{i-1/2}^*) \right).$$

The lack of accuracy in the internal energy computation resulting from the present scheme is not so crucial. The internal energies will be used only to estimate the phase's pressure at the end of the hyperbolic step, before the relaxation one. The relaxation step will give a first correction to the internal energies, in agreement with the second law of thermodynamics. A second correction will be made with the help of the total mixture energy. The details of these two steps are described in the next two subsections.

The method is extended in a straightforward manner to multi-dimensions by a finite volume method able to deal with structured and unstructured meshes, see [4] for details. Dependent variables are defined at cell centroids and fluxes, assumed constant along each cell face during a time interval, are determined as the HLLC approximate Riemann solution between the "left" and "right" cell states separated by the cell face.

### 3.3 Relaxation step

This step is of major importance to fulfill interface conditions in *non-uniform* velocity and pressure flows. It also forces the solution of the 6-equation model to converge to that of the 5-equation model. In the relaxation step we must solve

$$\frac{\partial \alpha_1}{\partial t} = \mu(p_1 - p_2)$$

$$\frac{\partial \alpha_1 \rho_1 e_1}{\partial t} = -p_1 \mu(p_1 - p_2)$$

$$\frac{\partial \alpha_2 \rho_2 e_2}{\partial t} = p_1 \mu(p_1 - p_2)$$

$$\frac{\partial \alpha_1 \rho_1}{\partial t} = 0$$

$$\frac{\partial \alpha_2 \rho_2}{\partial t} = 0$$

$$\frac{\partial \rho u}{\partial t} = 0$$

$$\frac{\partial \rho E}{\partial t} = 0$$

with  $p_1 = \frac{Z_2 p_1 + Z_1 p_2}{Z_1 + Z_2}$  and in the limit  $\mu \rightarrow +\infty$ .

After some manipulations the internal energy equations become

$$\frac{\partial e_1}{\partial t} + p_1 \frac{\partial v_1}{\partial t} = 0 ,$$

$$\frac{\partial e_2}{\partial t} + p_1 \frac{\partial v_2}{\partial t} = 0 .$$

This system can be written as an integral formulation

$$e_k - e_k^0 + \hat{p}_{1k} (v_k - v_k^0) = 0$$

$$\text{where } \hat{p}_{1k} = \frac{1}{v_k - v_k^0} \int_0^{\Delta t} p_1 \frac{\partial v_k}{\partial t} dt .$$

Determination of pressure averages  $\hat{p}_{1k}$  must be done in agreement with thermodynamic

considerations. Summing the internal energy equations gives

$$Y_1 e_1 - Y_1 e_1^0 + Y_2 e_2 - Y_2 e_2^0 + \hat{p}_{11} (Y_1 v_1 - Y_1 v_1^0) + \hat{p}_{12} (Y_2 v_2 - Y_2 v_2^0) = 0 .$$

The mixture mass equation can be written as

$$(Y_1 v_1 - Y_1 v_1^0) + (Y_2 v_2 - Y_2 v_2^0) = 0 .$$

Using these relations the mixture energy equation becomes

$$e - e^0 + (\hat{p}_{11} - \hat{p}_{12})(Y_1 v_1 - Y_1 v_1^0) = 0 .$$

In order that the mixture energy conservation be fulfilled it is necessary that  $\hat{p}_{11} = \hat{p}_{12} = \hat{p}_1$ .

Possible estimates are  $\hat{p}_1 = p_1^0$  or  $\hat{p}_1 = p^*$ , the initial and relaxed pressures respectively. These

estimates are both compatible with the entropy inequality [9]. Regarding the choice of one or the other estimate, upon computation of the relaxed state the resulting difference in practical computations is negligible. The system to solve is thus composed of equations

$$e_k(p^*, v_k^*) - e_k^0(p_k^0, v_k^0) + \hat{p}_1 (v_k^* - v_k^0) = 0, \quad k = 1, 2$$

which involves 3 unknowns,  $v_k^*$  ( $k = 1, 2$ ) and  $p^*$ . Its closure is achieved using the saturation constraint

$$\sum_k \alpha_k = 1,$$

or

$$\sum_k (\alpha \rho)_k v_k = 1 .$$

Here the  $(\alpha \rho)_k$  are constant during the relaxation process. This system can be replaced by a single equation with a single unknown ( $p^*$ ). With the help of the EOS Eqn. (2) the energy equations become

$$v_k^*(p^*) = v_k^0 \frac{p^0 + \gamma_k p_{\infty k} + (\gamma_k - 1) \hat{p}_1}{p^* + \gamma_k p_{\infty k} + (\gamma_k - 1) \hat{p}_1} ,$$

and thus the only equation to solve (for  $p^*$ ) is

$$\sum_k (\alpha \rho)_k v_k(p^*) = 1 \tag{6}$$

Once the relaxed pressure is found, the phase's specific volumes and volume fractions are determined. The relaxed pressure cannot be used to advance the solution to the next time step because there is no guarantee that the mixture EOS or the mixture energy be in agreement with this relaxed pressure. In order to respect total energy and correct shock dynamics on both sides of the interface, the following correction is employed.

### 3.4 Reinitialization step

As the volume fractions have been estimated previously by the relaxation method, the mixture pressure can be determined from the mixture EOS based on the mixture energy which is known from the solution of the total energy equation. Because the mixture total energy obeys a conservation law, its evolution is accurate in the entire flow field and in particular at shocks. The mixture internal energy is defined as

$$e = Y_1 e_1(\rho_1, p) + Y_2 e_2(\rho_2, p) . \quad (7)$$

The mixture pressure  $p$  is determined by solving Eqn. (7). In the particular case of fluids governed by the stiffened gas EOS, the resulting mixture EOS is

$$p(\rho, e, \alpha_1, \alpha_2) = \frac{\rho e - \left( \frac{\alpha_1 \gamma_1 p_{\infty 1}}{\gamma_1 - 1} + \frac{\alpha_2 \gamma_2 p_{\infty 2}}{\gamma_2 - 1} \right)}{\frac{\alpha_1}{\gamma_1 - 1} + \frac{\alpha_2}{\gamma_2 - 1}} , \quad (8)$$

which relates mixture energy, density and volume fractions. This EOS is valid in pure (or nearly pure) fluids, and in the diffuse interface zone. The volume fraction has very weak variations in nearly pure fluids, so that the computed pressure is nearly exact on both sides of the interface. This guarantees correct and conservative wave dynamics on both sides of the interface. Inside the numerical diffusion zone of the interface, numerical experiments show that the method is accurate too, as the volume fractions used in the mixture EOS Eqn. (8) have a quite accurate prediction from the relaxation method. Once the mixture pressure is determined from Eqn. (8) the internal energies of the phases are reinitialized with the help of their respective EOS

$$e_k = e_k(p, \alpha_k \rho_k, \alpha_k) \quad (9)$$

before going to the next time step.

### 3.5 Summary

The numerical method can be summarized as follows:

- At each cell boundary solve the Riemann problem of Eqn. System (5) with favorite solver. The HLLC solver of Section (3.1) is recommended.
- Evolve all flow variables with the Godunov type method of Section (3.2)
- Determine the relaxed pressure and especially the volume fraction by solving Eqn. (6). The Newton method is appropriate for this task.
- Compute the mixture pressure with Eqn. (8).
- Reset the internal energies with the computed pressure with the help of their respective EOS Eqn. (9).
- Go to the first item for the next time step.

## 4. TESTS

### Bubble interaction

Multidimensional finite volume extension of the method described above is first validated against shock tube experiments of shock-bubble interaction. The experiment is one of those proposed in Layes and Le Métayer [19] where full description of the experimental setup is provided. The configuration under study consists in a shock wave propagating at Mach number 1.5 into air at atmospheric conditions and interacting with a helium bubble. The initial density of

air is  $\rho_{air} = 1.29 \text{ kg} \cdot \text{m}^{-3}$  and the initial density of helium is  $\rho_{helium} = 0.167 \text{ kg} \cdot \text{m}^{-3}$ . In the simulation both fluids are considered as ideal gases with polytropic coefficients  $\gamma_{air} = 1.4$  and  $\gamma_{helium} = 1.67$ . The initial configuration is represented in Figure 1. Computed results are compared with experimental ones in Figure 2.

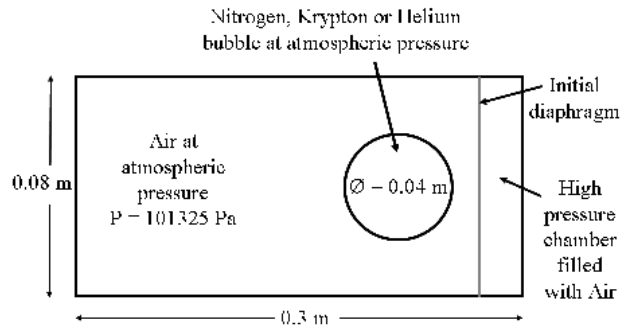


**Figure 1: Initial configuration of the interaction shock - bubble.**

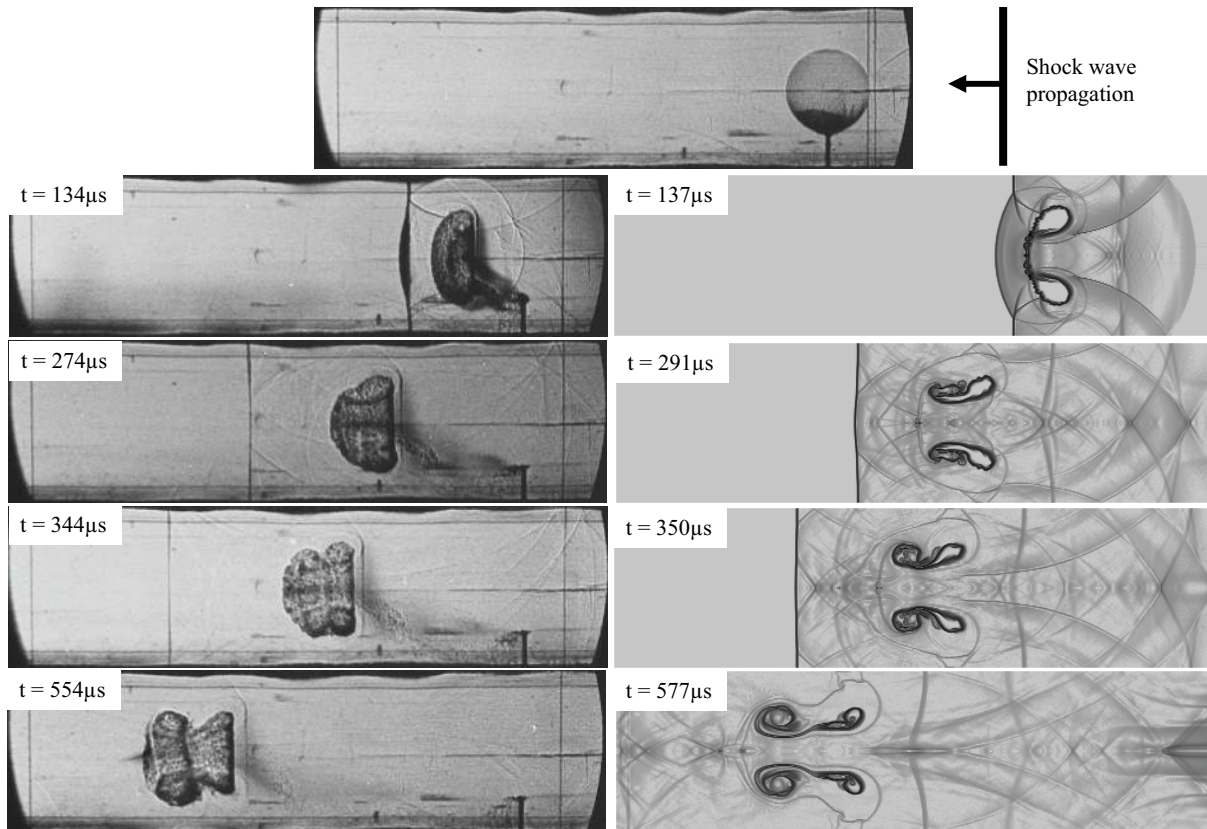


**Figure 2: Shock-bubble interaction test. Experimental results (left) and computed results (right) are compared at different times. Because of the difference in gas properties, the transmitted shock wave is faster than the incident one in air. Pressure and density gradients induce vorticity generation which develops at long time scale.**

### Cavitating Richtmyer-Meshkov instability (RMI)

To further illustrate the methods capabilities a 2D test involving a RMI is considered. As the liquid is not pure, new interfaces will appear during the development of the instability, due to cavitation effects. The shape of the resulting interface and the entire flow field show a non-conventional behavior, that was never computed before, as the model and method must deal with liquid gas interfaces and dynamic appearance of gas pockets in severe conditions. The left part of the computational domain is filled with nearly pure water and the right part with nearly pure gas. They are initially separated by a curved interface. It is a portion of circle with 0.6 meter radius centered at  $x = 1.2$  m,  $y = 0.5$  m. The physical domain is 3 m long and 1 m high. The mesh contains 900 cells along x-direction and 400 cells along y-direction. Both water and gas have an initial velocity of  $-200$  m/s. Top, bottom and left boundaries are treated as solid walls. The initial density of water is  $\rho_{water} = 1000$   $kg \cdot m^{-3}$  and the stiffened gas EOS parameters are  $\gamma_{water} = 4.4$  and  $p_{\infty, water} = 6.10^8$  Pa. The initial density of gas is  $\rho_{gas} = 100$   $kg \cdot m^{-3}$  and EOS parameters are  $\gamma_{gas} = 1.8$  and  $p_{\infty, gas} = 0$  Pa. The left chamber contains a very small volume fraction of gas  $\alpha_{gas} = 10^{-6}$  and the right chamber contains a very small volume

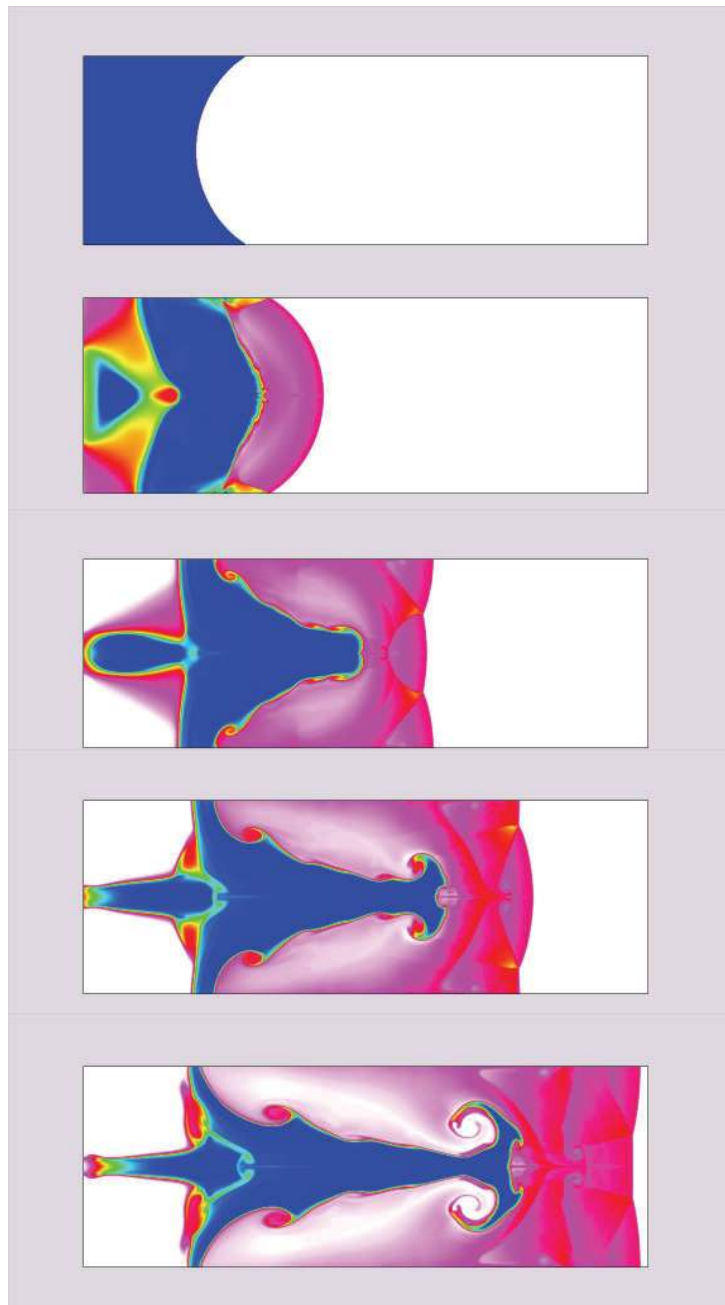
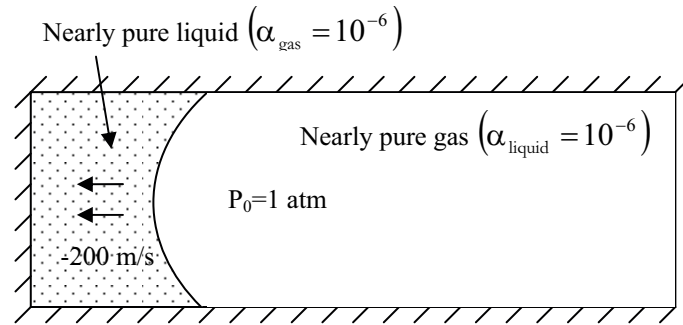


**Figure 1. Configuration and mixture density contours at 0.0, 1.9, 3.9, 5.8, and 7.8 ms. Blue is high density, white is low, and others colors are intermediate.**



fraction of water  $\alpha_{water} = 10^{-6}$ . The initial configuration and results are presented in Figure 3.

When the flow impacts the left wall, a right-facing shock propagates in the domain through the water/gas discontinuity. A conventional RMI appears first. Then expansion waves are produced as the jet elongates. It results in expanded zones near the solid boundary where gas inhomogeneities grow, producing dynamic appearance of gas pockets. As the pressure is very low in these zones, the jet dynamics is modified compared to conventional RMI with pure fluids. The various gas pockets near the solid boundary and in the jet core are clearly visible in Figure 4 where the gas volume fraction is shown. Relaxation terms present in the volume fraction and energy equations are responsible for the dynamic appearance of these gas pockets.

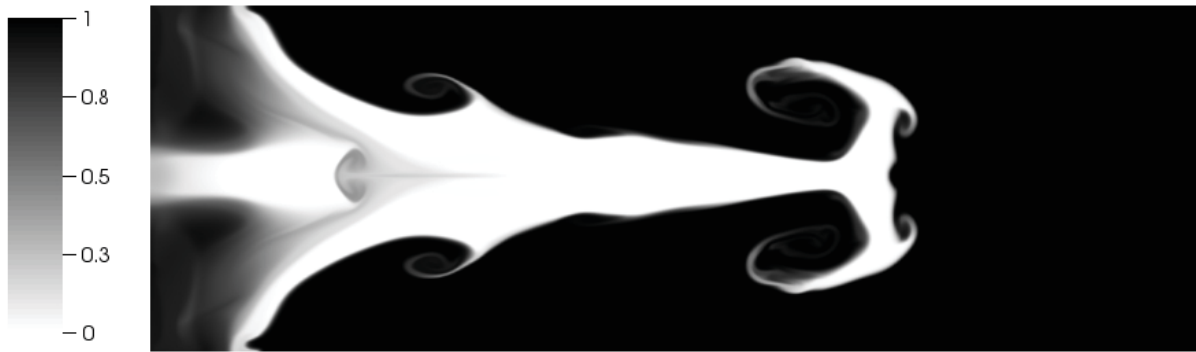


**Figure 4: Water-gas Richtmyer-Meshkov instability. Volume fraction contours of gas are shown at time  $t=8.6$  ms. The gas volume fraction increase into the liquid jet and near the solid wall boundary. The spike shape is also modified.**

The link between the 6-equation model and conventional barotropic cavitating flows that are the most popular in cavitation modeling is detailed in [4]. These models are composed of one or two mass conservation equations and one momentum equation. They consist in hyperbolic systems of conservation laws. These models involve an important difficulty related to the non-monotonic behavior of the sound speed versus volume fraction [13, 20, 14]. It is thus interesting to examine how the various ingredients developed in the context of the 6-equation model can be used for these barotropic models in order to solve this difficulty.

## 5. SUMMARY AND CONCLUSIONS

A relaxation hyperbolic model with 6 equations was presented to solve interface problems, flashing or cavitating flows and shocks into multiphase mixtures. This model considerably simplifies the numerical approximation of the 5-equation model of Kapila et al. [1]. A simple, efficient and robust algorithm was presented to solve the relaxation model. The various ingredients employed in this method are general enough to consider future extensions to problems involving complex physics such as surface tension and heat and mass transfer between the phases.

Using the fractional step method to calculate this type of initial value problem consisting of different kinds of physics with multiple time-scales, some of which should be treated implicitly, requires some precautionary measures to avoid splitting and conditioning errors. We are led to conclude that a fully implicit treatment may be advantageous. In the future we will investigate this approach to allow integration over the fast time scales for slow speed flows. We anticipate that using a Jacobian-Free Newton-Krylov method [21, 22] with physics based preconditioning will allow tightly coupled solutions of the multiphysics phenomena inherent in nuclear reactor core applications.

## ACKNOWLEDGMENTS

The authors acknowledge the U.S. Department of Energy, Office of Nuclear Energy for partially funding the preparation of this manuscript through the Idaho National Laboratory under DOE Idaho Operations Office Contract DE-AC07-05ID14517.

## REFERENCES

1. Kapila A.K., Menkoff R., Bdzil J.B., Son S.F., and Stewart D.S., "Two-phase modeling of deflagration-to-detonation transition in granular materials: Reduced equations," *Physics of Fluids* **13** (10) (2001) 3002-3024.
2. Saurel R., Petitpas F., and Abgrall R., "Modelling phase transition in metastable liquids: application to cavitating and flashing flows," *J. of Fluid Mech.* **607** (2008) 313-350.
3. *Two-phase convective flow modelling workshop*, Organized by the Societe Hydrotechnique de France (SHF) and the International Association of Hydraulic Engineering and Research (IAHR) under sponsorship of Societe Francaise des Thermiciens (SFT), CEA, AREVA, EDF, and AFM. Held in Grenoble, France, September 8-9, 2008.
4. Saurel R., Petitpas F., and Berry R.A., "Simple and efficient relaxation methods for interfaces separating compressible fluids, cavitating flows and shocks in multiphase mixtures," *J. Comp. Phys.* **228** (2009) 1678-1712.
5. Baer M.R., Nunziato J.W., "A two-phase mixture theory for the deflagration-to-detonation transition (DDT) in reactive granular materials," *Int. J. Multiphase Flow* **12** (6) (1986) 861-889.
6. Stewart H.B., Wendroff B., "Two-phase flow: models and methods," *J. Comp. Phys.* **56** (3) (1984) 363-409.
7. Murrone A., Guillard H., "A five equation reduced model for compressible two phase problems," *J. Comp. Phys.* **202** (2) (2005) 664-698.
8. Abgrall R., Perrier V., "Asymptotic expansion of a multiscale numerical scheme for compressible multiphase flows," *SIAM J. Multiscale and Modeling and Simulation* **5** (2006) 84-115.
9. Saurel R., Franquet E., Daniel E., Le Metayer O., "A relaxation-projection method for compressible flows. Part 1. The numerical equation of state for the Euler equations," *J. Comp. Phys.* **223** (2) (2007) 822-845.

10. Petitpas F., Franquet E., Saurel R., Le Metayer O., “A relaxation-projection method for compressible flows. Part 2. The artificial heat exchange for multiphase shocks,” *J. Comp. Phys.* **225** (2) (2007) 2214-2248.
11. Wood A.B., *A Textbook of Sound*, Bell and Sons Ltd., London, 1930.
12. Toro E.F., *Riemann Solvers and Numerical Methods for Fluid Dynamics*, Springer-Verlag, Berlin, 1997.
13. Koren B., Lewis M.R., van Brummelen E.H., van Leer B., “Riemann-problem and level-set approaches for homentropic two-fluid computations,” *J. Comp. Phys.* **181** (2002) 654-674.
14. Sinibaldi E., “Implicit preconditioned numerical schemes for the simulation of three-dimensional barotropic flows,” *Ph.D. Thesis*, Scuola Normale Superiore di Pisa, Italy, 2006.
15. Saurel R., Gavriluk S., Renaud F., “A multiphase model with internal degrees of freedom: application to shock-bubble interaction,” *J. Fluid Mech.* **495** (2003) 283-321.
16. Saurel R., Le Metayer O., Massoni J., Gavriluk S., “Shock jump relations for multiphase mixtures with stiff mechanical relaxation,” *Shock Waves* **16** (3) (2007) 209-232.
17. Davis S.F., “Simplified second order Godunov type methods,” *SIAM J. Sci. Stat. Comput.* **9** (1988) 445-473.
18. Hou T.Y., Le Floch P., “Why non-conservative schemes converge to the wrong solution: error analysis,” *Math. of Comp.* **62** (1994) 497-530.
19. Layes G., Le Metayer, “Quantitative numerical and experimental studies of the shock accelerated heterogeneous bubbles motion,” *Phys. of Fluids* **19** (2007) 042105.
20. Coutier-Delgosha O., Fortes-Patella R., Reboud J.L., Hakimi N., Hirsch C., “Stability of preconditioned Navier-Stokes equations associated with a cavitation model,” *Comp. and Fluids* **34** (2005) 319-349.
21. Knoll D.A., Mousseau V.A., Chacon L., Reisner J., “Jacobian-free Newton-Krylov methods for the accurate time integration of stiff wave systems,” *J. Sci. Comput.* **25** (1/2) (2005) 213-230.
22. Knoll D.A., Keyes D.A., “Jacobian-free Newton-Krylov methods: a survey of approaches and applications,” *J. Comp. Phys.* **193** (2004) 357-397.